

Effect of surface site on the spin state of first-row transition metals adsorbed on MgO: Embedded cluster model and hybrid density functional theory calculations

Elizabeth Florez,¹ Fanor Mondragón,¹ Patricio Fuentealba,² and Francesc Illas³

¹*Instituto de Química, Universidad de Antioquia, A.A. 1226, Medellín, Colombia*

²*Departamento de Física, Universidad de Chile, Las Palmeras 3425, Ñuñoa, Santiago, Chile*

³*Department de Química Física i Institut de Química Teòrica i Computacional (IQTCUB), Universitat de Barcelona, C/Martí i Franquès 1, E-08028 Barcelona, Spain*

(Received 2 May 2008; revised manuscript received 4 July 2008; published 20 August 2008)

The interaction of first-row transition-metal atoms with low-coordinated oxygen atoms and oxygen vacancies of the MgO surface at low coverage has been studied systematically using an embedded-cluster model approach and hybrid density functional theory calculations. It was found that the interaction with these defects is much stronger than with the regular sites but in general insufficient to change the number of unpaired electrons in the free metal atom. Nevertheless, the larger interaction at these sites reduces the energy required to switch from high spin to low spin. These findings are in agreement with previous work on the adsorption of transition-metal atoms on regular anionic sites of the MgO(001) surface. Our results show that the spin state of adsorbed metal atoms on oxide supports needs to be explicitly taken into account.

DOI: 10.1103/PhysRevB.78.075426

PACS number(s): 73.20.At, 71.15.Mb, 68.47.Gh

I. INTRODUCTION

Transition metal atoms, clusters and nanoparticles supported on various oxide surfaces have broad applications in different industrial processes, especially in catalysis,^{1–4} but also in other equally important and relevant technologies.^{5–7} This has stimulated active research on the fundamental understanding of structural and electronic properties of the metal—support interface either from experimental or theoretical points of view.^{8–10} From the experimental side, considerable progress has been achieved with the study of the electronic and geometric properties of supported metal particles.¹¹ More recently, sample manipulation at the atomic scale has enabled the preparation and analysis of individual atoms, dimers and trimers of Pd supported on MgO(001)¹² and of individual Au atoms on MgO.^{13,14} Theoretical studies have also reached a point where the structure of rather large supported clusters can be determined using first-principles methods,^{15–20} thus extending earlier work based on the use of pair potentials.²¹ A number of theoretical studies using either cluster or periodic models have chosen MgO(001) as representative of a nonreducible substrate and focused on the strength of the metal-oxide interaction, the nature of the chemical bond between transition metals and this perfect oxide surface, on the electronic properties of the adsorbed atoms^{22–29} and, more recently on the metal/oxide interface Cu(MgO(001) and Ni/Mg(001) systems.³⁰ Yudanov *et al.*²⁷ have studied the low coverage regime and classified the transition-metal atoms into two main groups, one containing atoms that tend to form relatively strong bonds with the surface oxygen anions of MgO (Ni, Pd, Pt, and W), and one containing atoms that have weak interaction with the MgO surface (Cr, Mo, Cu, Ag, and Au). A recent comprehensive article by Cinquini *et al.*³¹ includes a discussion of the main bonding mechanism and how morphology, presence of defects, doping and functionalization, redox properties, and substrate thickness affect the properties of supported metal atoms and nanoparticles.

An important consequence of the interaction between transition-metal atoms or clusters with MgO(001) at very

low coverage is that it may induce changes in the electronic states of the supported particle or adsorbed atom.^{32,33} The effect of the substrate on the electronic states of the adsorbate is easily analyzed in the case of first-row transition metal atoms. For the isolated atoms except Cr, the electronic ground state is a $d^n s^2$ whereas upon adsorption the electronic ground state becomes $d^{n+1} s^1$. At the same time, a concomitant change is induced in the total spin (particularly, on the magnetic moment) of the adsorbed atom. Markovits *et al.*³⁴ found that the energy required to change the atomic state from high to low spin of first-row transition metals (Ti, V, Cr, Fe, Co, and Ni) supported on the MgO (100) surface is lower than that for of the isolated atoms, leading in some cases to a change in the multiplicity of the ground state with respect to the free atoms such as V, Ni, and Co.

The above discussion refers to the interaction of transition-metal atoms with regular sites of the perfect MgO(001) surface. However, it is well known that point defects, in particularly oxygen vacancies, play a key role in defining the properties of adsorbed metal atoms and clusters. For instance, vacancies bind large clusters strongly enough to trap them.³⁵ The important role of oxygen vacancies has been stressed by Pacchioni, who has termed them “invisible agents” of surface chemistry.³⁶ Nevertheless, little is known about the influence of these point defects on the relative energy of the low lying states and, in particular, of the energy required to switch from low spin to high spin. In the case of Ni atoms adsorbed on oxygen vacancies at low coverage, the interaction energy between the metal and the support is much larger than on regular sites, resulting in a diamagnetic adsorbed species, and the energy required to reach the high-spin state increases in opposition to the trend found for the first-row transition-metal atoms on the regular sites of the perfect MgO(001) surface.³⁷ The fact that the interaction with different sites induces qualitatively different changes on the energy required to switch from low spin to high spin may have technological consequences and merits a more detailed study. This is the main goal of the present paper.

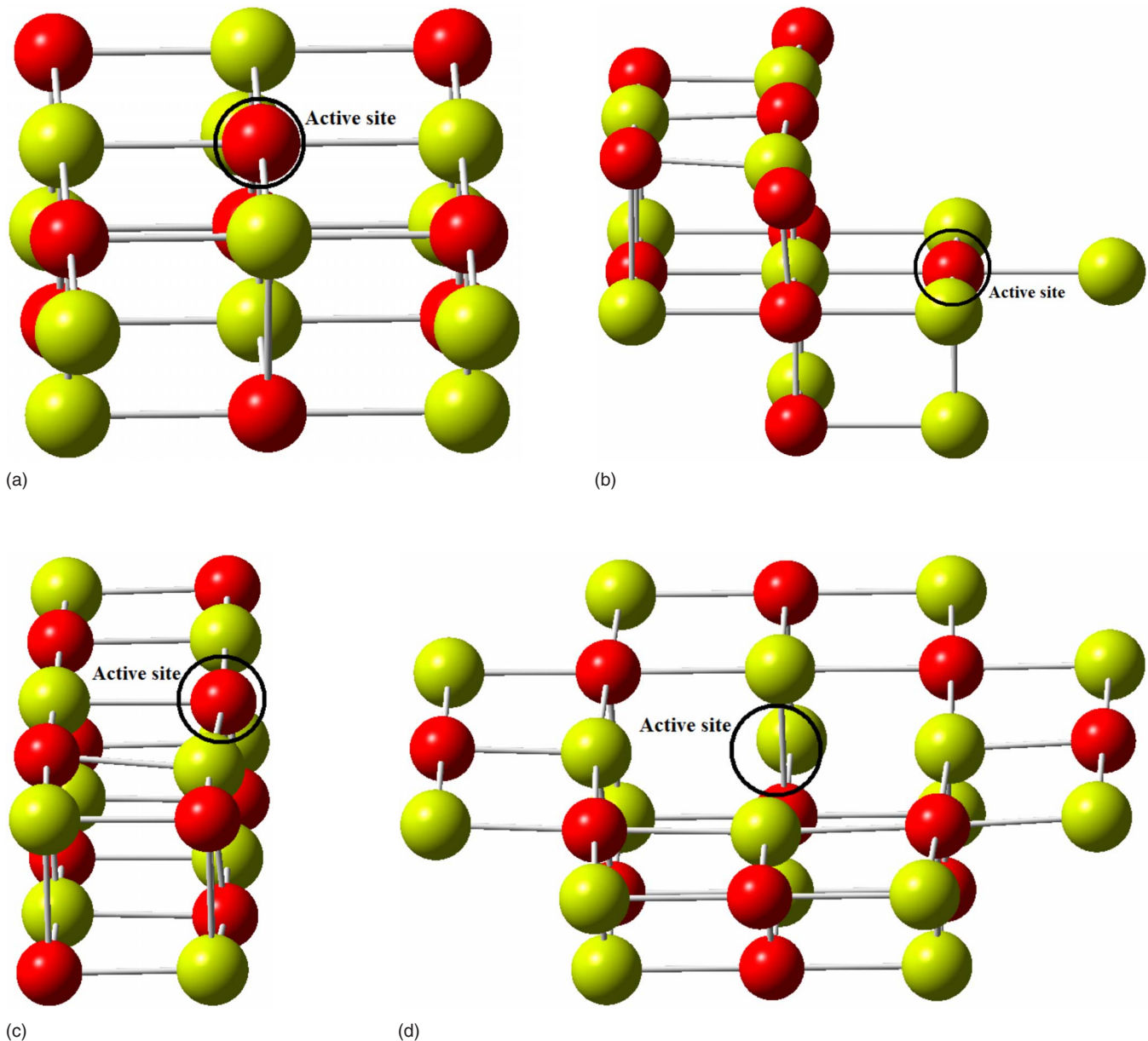


FIG. 1. (Color online) Schematic depiction of the quantum-mechanical region of the embedded-cluster models use to represent (a) the regular terrace site, (b) the step site, (c) the edge site, and (d) the F_S oxygen vacancy site.

II. SURFACE MODELS AND COMPUTATIONAL DETAILS

The interaction of first-row transition-metal (TM) atoms with various sites of the MgO surface at low coverage has been studied by means of an embedded-cluster approach, a natural choice when focusing on low coverage situations and/or involving point defects. Regular terrace, step, edge, and F_S surface oxygen vacancy (arising from the removal of one neutral O and leaving two electrons in the cavity) sites have been considered and modeled by appropriate embedded clusters containing a quantum mechanical (QM) and a classical region.^{28,29,34,38} Here, it is worth pointing out that F_S vacancies are most numerous at step edges and the model used here refers to a terrace F_S center. This is used to explore the effect of a larger value of the interaction energy on the energy difference between low- and high-spin state of the

adsorbed TM atom. The QM region is divided into two main parts, QM1 and QM2. QM1 contains the Mg and O atoms, which are explicitly treated by an appropriate quantum chemical method, whereas QM2 contains a set of total ion model potentials (TIMP) representing all Mg^{2+} cations which are directly in contact to any of the oxygen atoms in the QM1 region. The classical region contains an array of point charges (PC) forming a unit cell of 1.2 nm introduced to account for the long-range Madelung potential. The TIMPs and point charges ($\text{PC} = \pm 2$) are located at the lattice positions, which were taken from the experimentally determined MgO bulk structure. QM1 regions for terrace, step, edge, and F_S center are Mg_9O_9 , two different $\text{Mg}_{10}\text{O}_{10}$ clusters, and $\text{Mg}_{13}\text{O}_{12}$, respectively (Figs. 1). The TM atom has been placed above an anionic site of the MgO(100) surface, the most favorable adsorption site at regular terraces.^{27–29,39}

TABLE I. Experimental ground state (electronic configuration and lowest multiplet) and ground state (electronic configuration and number of unpaired electron) predicted by the B3LYP method.

	Experimental ground state	Electronic configuration	Calculated B3LYP ground state Number of unpaired electrons
Ti	...3d ² 4s ² (³ F)	...3d ² 4s ²	2
V	...3d ³ 4s ² (⁴ F)	...3d ³ 4s ²	3
Cr	...3d ⁵ 4s ¹ (⁷ S)	...3d ⁵ 4s ¹	6
Mn	...3d ⁵ 4s ² (⁶ S)	...3d ⁵ 4s ²	5
Fe	...3d ⁶ 4s ² (⁵ D)	...3d ⁶ 4s ²	4
Co	...3d ⁷ 4s ² (⁴ F)	...3d ⁷ 4s ²	3
Ni	...3d ⁸ 4s ² (³ F)	...3d ⁸ 4s ²	2

The QM1 region is described by explicit electronic structure calculations including all electrons of the atoms in this region while the QM2 contains just Mg effective core potential with a total charge of +2. The total energy of the QM region was calculated using density functional theory with the hybrid B3LYP exchange-correlation potential.⁴⁰ This ensures a correct description of the electronic ground state of first-row transition-metal atoms and a reasonable description of the energy difference between low lying electronic states with different spin multiplicity.³⁴ In addition, the B3LYP adsorption energies of transition-metal atoms on regular sites of the MgO(001) are rather independent on the basis set.^{29,34} Standard Gaussian type orbital basis sets have been used to expand the Kohn-Sham electron density. A 6–31 G(d,p) basis set was used for selected surface Mg and O atoms close to the adsorption center whereas the 3–21 G(d,p) basis set was used for the remaining atoms in the QM1 region. The LANL2 effective core potential with its corresponding LANL2DZ basis set was used for the transition-metal atoms. Geometries of the adsorbed metal atom and MgO atoms in the QM1 directly interacting with it have been fully optimized while the rest of the atoms in the QM1 and QM2 regions are kept fixed at the bulk value.

All electronic structure calculations have been carried out within the spin unrestricted implementation of the Kohn-Sham scheme using GAUSSIAN 03 suite of programs.⁴¹

III. RESULTS AND DISCUSSION

The experimental and calculated ground state of the first-row transition-metal atoms in the gas phase are shown in Table I. Note that because of the use of a single Slater determinant as in the standard Kohn-Sham implementation of density functional theory, it is not possible to assign space and spin symmetry to an open shell solution.^{42–44} The multiplet structure can be recovered by making use of the sum rule as suggested in the currently classical articles of Bennet and Bagus⁴⁵ or Rauk, Baerend, and Ziegler.⁴⁶ For the present purposes, however, it is sufficient to rely on the electronic ground-state configuration. At this qualitative level the B3LYP properly describes ground-state electronic configura-

tion of the isolated atoms as already shown in previous work.³⁴

Next, we briefly describe the general trends corresponding to the adsorption energy of the first-row transition-metal atoms in the terrace, step, edge, and F_s sites. The adsorption energies have been calculated as

$$E_{\text{ads}} = E(\text{TM}) + E(\text{MgO}) - E(\text{TM/MgO}) \quad (1)$$

where $E(\text{TM})$ is the energy of the isolated free transition-metal atom in its ground state, $E(\text{MgO})$ is the energy of the cluster model, and $E(\text{TM/MgO})$ the energy of the super system in the electronic ground state. For the F_s oxygen vacancy, with two electrons in the cavity, we considered a closed-shell low-spin state. Positive values of the adsorption energy correspond to an exothermic process. The adsorption energies at terrace sites calculated by means of a cluster model have found to be rather independent of the cluster size provided that an adequate embedding scheme is used.^{28,29} However, one must admit that this is not fully guaranteed when dealing with other properties or other sites. Nevertheless, there is enough evidence to expect that the general qualitative trends will remain upon increasing the clusters size. For instance, embedded cluster for F_s centers at terraces, steps, and corners have been used to study the excitation energies of the trapped electrons and predicted values which have been later confirmed by experiment.⁴⁷ Similar cluster modes have been used to interpret the optical spectra of supported Cu atoms and nanoclusters³³ as well as to assign point defects in MgO nanocrystals.^{48,49} Therefore, it is expected that the cluster models used in this work provide meaningful results for the properties of interest. It is also clear that the calculated values are also affected by the choice of the exchange-correlation potential and by the basis set superposition error used, although the latter can be corrected by standard methods. In any case, results reported in the present work have not been corrected by the basis set superposition error because the main goal here is to analyze both the energy required to switch from high-spin to low-spin state and the trends along the series as well as, for each transition-metal atom, along the type of surface site. These trends will not be affected by including such correction.

First of all, it is interesting to explore the electronic configuration of the adsorbed metal atoms which are summarized in Table II. For the interaction of the first-row transition-metal atoms with the regular site, the overall description is very close to those reported in previous work using a similar approach. Thus, the only appreciable change with respect to the free atom is the hybridization between 4s and 3d orbitals with negligible contribution of the 4p subshell and no appreciable charge transfer. This is clear from the new results presented in Table II which have been obtained from a natural bond orbital (NBO) population analysis.⁵⁰ This analysis reveals that, for the interaction with regular terrace sites, the total number of electrons on the adsorbed atom is very close to that obtained for the free atom. In all cases involving regular terrace sites, the electronic ground state of the adsorbed atom tends to maintain the spin state of the free atom except for the case of Ni and Co where the electronic ground state of the adsorbed atom

TABLE II. Electron configuration (EC) and total number of electrons (N_e) for first-row transition-metal atoms (Ti to Ni) adsorbed on different sites of the MgO(100) surface as predicted from a NBO population analysis.

Atom	Site									
	Free		Regular		Edge		Step		F_S	
	EC	N_e	EC	N_e	EC	N_e	EC	N_e	EC	N_e
Ti	$4s^23d^2$	4	$4s^{1.71}3d^{2.35}4p^{0.03}$	4.09	$4s^{1.61}3d^{2.51}4p^{0.02}$	4.14	$4s^{1.52}3d^{2.64}4p^{0.08}$	4.24	$4s^{1.62}3d^{2.80}4p^{0.26}$	4.68
V	$4s^23d^3$	5	$4s^{1.65}3d^{3.40}4p^{0.01}$	5.06	$4s^{1.52}3d^{3.55}4p^{0.02}$	5.09	$4s^{1.42}3d^{3.74}4p^{0.07}$	5.23	$4s^{1.41}3d^{4.05}4p^{0.19}$	5.65
Cr	$4s^13d^5$	6	$4s^{1.00}3d^{4.98}4p^{0.02}$	6.00	$4s^{1.45}3d^{4.59}4p^{0.03}$	6.07	$4s^{1.49}3d^{4.60}4p^{0.08}$	6.17	$4s^{1.40}3d^{4.93}4p^{0.24}$	6.57
Mn	$4s^23d^5$	7	$4s^{1.82}3d^{5.15}4p^{0.02}$	7.00	$4s^{1.35}3d^{5.70}4p^{0.04}$	7.03	$4s^{1.57}3s^{5.37}4p^{0.11}$	7.05	$4s^{1.91}3d^{5.16}4p^{0.16}$	7.23
Fe	$4s^23d^6$	8	$4s^{1.59}3d^{6.42}4p^{0.03}$	8.04	$4s^{1.49}3d^{6.40}4p^{0.09}$	8.01	$4s^{1.52}3d^{6.47}4p^{0.11}$	8.1	$4s^{1.54}3d^{6.86}4p^{0.35}$	8.75
Co	$4s^23d^7$	9	$4s^{1.16}3d^{7.85}4p^{0.04}$	9.05	$4s^{1.41}3d^{7.53}4p^{0.07}$	9.01	$4s^{1.36}3d^{7.63}4p^{0.12}$	9.11	$4s^{1.59}3d^{7.98}4p^{0.35}$	9.92
Ni	$4s^23d^8$	10	$4s^{0.94}3d^{9.15}5p^{0.02}$	10.11	$4s^{1.36}3d^{8.55}4p^{0.08}$	9.99	$4s^{1.25}3d^{8.75}4p^{0.12}$	10.12	$4s^{1.43}3d^{9.71}4p^{0.01}$	11.15

represents a qualitative change with respect to the free-atom situation mentioned by Markovits *et al.*³⁴ This is in agreement with a bonding interaction between the transition-metal atom and the regular anionic sites dominated by the polarization of the transition-metal atom induced by the presence of the underlying ionic substrate.^{27–29} On the other hand, the interaction of the transition-metal atoms with low-coordinated anionic sites and with F_S centers results in stronger adsorption energies.^{22,37,51–55} The effect is greater when the interaction takes place above the low-coordinated sites, whereas the effect on the electronic structure of the adsorbed atom is larger when the interaction takes place above the F_S center; see Tables II and III. This may be explained by the following argument; the interaction above low-coordinated sites faces a smaller Pauli repulsion because the oxygen anion electron density is more delocalized and results in a larger value of the calculated adsorption energy. The interaction above the F_S center is different, since the final adsorption energy is not as large as in the case of the step or edge sites (Table III) but produces a larger change in the atomic electron density (Table II). The increased adsorption energy is accompanied by notable changes in the electronic configuration of the adsorbed metal which is progressively changed by a charge transfer from the anionic sites mainly to the $3d$ shell but also with an increasing participation of the $4p$ or-

TABLE III. Calculated B3LYP adsorption energies (eV) for the TM atoms supported on an anionic site of the terrace, step, edge, and F_S sites of MgO. The number of unpaired electrons for the electronic ground state is given in parenthesis to compare to results for the free atom also given in Table I.

TM	Site			
	Terrace	Step	Edge	F_S
Ti (2)	1.21 (2)	4.16 (2)	2.60 (2)	1.26 (2)
V (3)	1.01 (3)	3.93 (3)	2.48 (3)	1.50 (5)
Cr (6)	0.40 (6)	2.72 (4)	1.78 (4)	1.29 (6)
Mn (5)	0.60 (5)	2.78 (5)	1.56 (5)	0.49 (5)
Fe (4)	0.81 (4)	3.22 (4)	2.08 (4)	1.32 (4)
Co (3)	0.80 (1)	3.42 (3)	2.15 (3)	2.23 (1)
Ni (2)	1.33 (0)	3.34 (2)	1.95 (2)	2.48 (0)

bitals. The resulting adsorbed metal atom and almost O^- surface ion can be regarded as an effective ion pair which is held together by covalent interaction and stabilized by the long-range Madelung potential.

Concerning the calculated adsorption energies, the values for the interaction above the regular site strongly agree with previous work although the coincidence may be fortuitous since the present values have been obtained with the B3LYP exchange-correlation potential and with an embedded-cluster model whereas those reported by Markovits *et al.*³⁴ were obtained using a periodic slab model and the PW91 potential. Nevertheless, it is interesting to note that the present adsorption energies (B3LYP) for Ni, Co, Fe, Mn, and Cr compare well with the BP96 and RPBE values reported recently in a systematic study by Neyman *et al.*⁵⁵ However, the B3LYP values are always somewhat smaller in line with previous findings.^{28,29} The values corresponding to the interaction with anion sites at step and edges follow the same trend as for the interaction on the terrace sites. The adsorption energy first decreases from Ti to Cr and then increases from Mn to Co with Co and Ni exhibiting a different trend which may be understood by the change in the spin state when the interaction involves a regular site. Overall, the adsorption energy is largest for the step site although the one corresponding to the edge is also, in all cases, larger than the one corresponding to the regular site, a result that is in line with experimental findings showing that nucleation of metals on oxide supports takes place preferentially at line defects.^{56–58} The trend is, however, different for the interaction above the F_S site, a result also found by Neyman *et al.*,⁵⁵ and this has implications on the high- to low-spin transition energy as discussed below.

Now we come to the central point of the present work, namely, the effect of adsorption site on the high- to low-spin transition energies. The B3LYP calculated high- to low-spin (ΔE^{H-L}) transition energies are summarized in Table IV and Fig. 2. A negative sign indicates that the ground state corresponds to the low-spin state. It is important to point out that the B3LYP calculated transition energies for the isolated transition-metal atoms have an average error of 0.4 eV (Ref. 34) and most of the values in Table IV follow in this range. Nevertheless, the important point here is the trend when moving the transition-metal atom from one site to another

TABLE IV. Calculated B3LYP high- to low-spin (ΔE^{L-S}) transition energies (in eV) for the TM atoms supported on an anionic site of the terrace, step, edge and F_S sites of MgO. A negative number indicates a change in the spin state of the adsorbed metal atom with respect to the free atom.

TM	Site			F_S
	Terrace	Step	Edge	
Ti	0.84	0.83	0.44	1.42
V ^a	-0.07	-0.66	-0.67	0.13
Cr	0.14	-0.26	-0.62	0.02
Mn	1.36	1.30	1.55	0.41
Fe	1.19	0.91	1.00	0.03
Co	-0.06	0.52	0.33	-0.07
Ni	-0.02	0.59	0.13	-0.38

^aFor V the high spin state considered is a sextuplet arising from the $4s^1 3d^4$ electronic configuration.

and this is likely to be correct at least qualitatively. Moreover, quick inspection of Table II shows that in most cases the number of unpaired electrons for the adsorbed atom remains the same as in the free atom. Therefore, one may expect that at very low coverage adsorbed transition-metal atoms will display a net magnetic moment even when the interaction takes place above low coordinate anions or above oxygen vacancies. This is quite a new and unexpected result since one would expect that a larger value of the interaction energy will produce a total quench of the spin in the adsorbed metal atom. Nevertheless, the analysis of Fig. 2 clearly shows that there is a change in the transition energy required to switch from high spin to low spin (ΔE^{H-L}), which is induced by the underlying oxide support surface. In almost all cases the energy required to go from the high spin to low spin decreases when the support is present and in a few cases such as V, Co, and Ni on terrace sites and Co and Ni on F_S

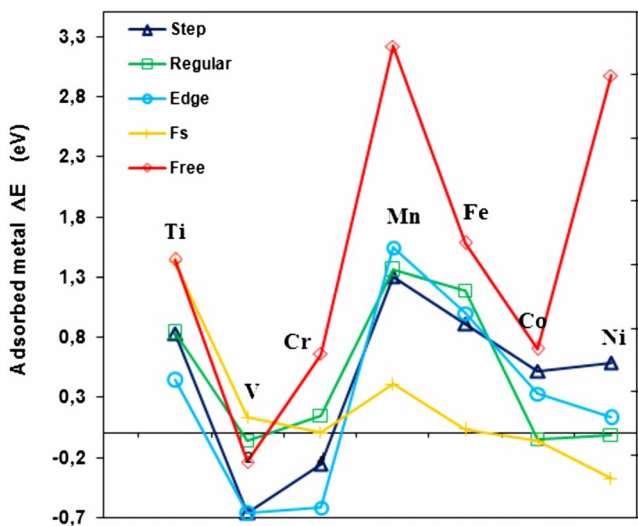


FIG. 2. (Color online) Calculated B3LYP high- to low-spin transition energies for first-row transition-metal atoms adsorbed on various regular, low-coordinated and defect sites of the MgO surface.

sites, the low-spin state becomes the ground state. Note that for Co and Ni, the results on these two sites are also in agreement with previous findings.^{34,55} A low-spin electronic ground state is also found for the interaction of V and Cr at the low-coordinated sites (step and edge) and this coincides with the fact that the metal-support interaction is the largest. These results seem to indicate that partial spin quenching will only take place in situations leading to a large enough adsorption energy. Notice, however, that in order to compare with previous work³⁴ and with the case with V at the F_S center (see below) the high spin state of V is a sextuplet state arising from the $4s^1 3d^4$ electronic configuration which is the ground state for the PW91 functional. In any case, the trend emerging from the present model calculations indicates that the metal-support interaction tends to stabilize the low-spin state with respect to the isolated atom, the low-spin state becoming the ground state only in some cases (Co and Ni at terrace and F_S sites but not at step and edge and Cr at step and edge but not at terrace and F_S).

The interaction with the F_S center merits a separate discussion since results show that in almost all cases ΔE^{H-L} the transition energy exhibits the largest decrease. In these cases it is clear that the low-spin state is more favored because of the formation of a direct bond between the adsorbed transition-metal atom and the electronic levels corresponding to the oxygen vacancy electrons. Nevertheless, Ti and V are exceptions. For the adsorbed Ti and isolated atom the ΔE^{H-L} transition energies are 1.42 and 1.54 eV, respectively, which show almost no variation. This behavior can be easily understood in terms of the Hund rules since adsorbed Ti has a degenerate HOMO-1 which is composed mainly of the metal d_{yz} and d_{xz} orbitals thus stabilizing the triplet state. In the other adsorption site this situation is not present and the ΔE^{H-L} energy decreases. For the free V atom and also for the adsorbed one at the regular and low-coordinated sites, the ground state is a quadruplet arising from the $4s^2 3d^3$ configuration, as mentioned above. However, for the V atom at the F_S center, we find that the electronic ground state is a sextuplet arising from the $4s^1 3d^4$ configuration. This change has a chemical origin, the highest occupied molecular orbital (HOMO) has a strong antibonding character thus causing a larger destabilization of the V/F_S complex compared with sextuplet multiplicity.

IV. CONCLUSIONS

The interaction of first-row transition-metal atoms with regular, low-coordinated (step and edge) and oxygen vacancy sites of the MgO surface at low coverage has been studied in a systematic way using embedded-cluster models and a hybrid density functional theory approach with a focus on the electronic structure of the adsorbed atom and on the energy required to partially quench the total spin of the free atom. The interaction above low-coordinated anions is found to be substantially stronger than on the regular terrace sites, the final adsorption energy being two to three times larger. The interaction above the regular oxygen vacancy sites is also stronger than that at the regular terrace sites but generally smaller than for the interaction above low-coordinated

surface oxygen anions. This is in agreement with experimental evidence that nucleation takes place preferentially at these sites.⁵⁹ In spite of the enhanced interaction with the substrate, the adsorbed atomic electronic ground state tends to preserve the number of unpaired electrons as found in the case of the regular terrace sites. However, for the largest adsorption energy such as Cr at step and edge sites, a partial spin quench is observed.

To summarize, first-row transition-metal atoms on low coordinated and oxygen vacancies of the MgO surface tend to preserve the electronic configuration and number of unpaired electrons as in the free atom. Nevertheless, the larger interaction at these sites induces a reduction of the energy required to switch from high spin to low spin. In most cases, however, the decrease is not enough to even partially quench

the spin of the adsorbed atom. These findings are in line with previous results reported on the interaction with the regular terrace sites and show that the spin state of adsorbed metal atoms on oxide supports has to be explicitly considered.

ACKNOWLEDGMENTS

This study has been supported in part by the Spanish Ministry of Education and Science (Grants No. CTQ2005-08459-CO2-01 and No. UNBA05-33-001), the Generalitat de Catalunya (Grants No. 2005SGR00697 and No. 2005PEIR0051/69), the Fondecyt (Grants No. 3080033 and No. 1080184), and the Sostenibilidad Program of the University of Antioquia. E.F. would like to thank Colciencias and the University of Antioquia for financial support.

-
- ¹J. A. Anderson and M. Fernandez-Garcia, *Supported Metals in Catalysis* (Imperial College, London, 2005).
- ²C. T. Campbell, *Surf. Sci. Rep.* **27**, 1 (1997).
- ³C. R. Henry, *Surf. Sci. Rep.* **31**, 231 (1998).
- ⁴*Chemisorption and Reactivity on Supported Clusters and Thin Films*, NATO Advanced Studies Institute, Series E: Physics Vol. 331, edited by R. M. Lambert and G. Pacchioni (Kluwer, Dordrecht, 1997).
- ⁵M. Moseler, H. Häkkinen, and U. Landman, *Phys. Rev. Lett.* **89**, 176103 (2002).
- ⁶T. H. Lee and R. M. Dickson, *Proc. Natl. Acad. Sci. U.S.A.* **100**, 3043 (2003).
- ⁷S. Fukami, A. Ohno, and A. Tanaka, *Mater. Trans.* **45**, 2012 (2004).
- ⁸H. J. Freund, *Surf. Sci.* **500**, 271 (2002).
- ⁹A. Wieckoski, E. R. Savinova, and C. G. Vayenas, *Catalysis and Electrocatalysis at Nanoparticle Surfaces* (Dekker, New York, 2003).
- ¹⁰N. Lopez and F. Illas in *Supported Metals in Catalysis*, edited by J. A. Anderson and M. Fernandez-Garcia (Imperial College, London, 2005), Chap. 2, and references therein.
- ¹¹U. Heiz and W.-D. Schneider, in *Metal Clusters at Surfaces*, edited by K. H. Meiwes-Broer (Springer, Berlin, 2000), pp. 237–273.
- ¹²M. Sterrer, T. Risse, L. Giordano, M. Heyde, N. Nilus, H. P. Rust, G. Pacchioni, and H.-J. Freund, *Angew. Chem., Int. Ed.* **46**, 8703 (2007).
- ¹³M. Yulikov, M. Sterrer, M. Heyde, H. P. Rust, T. Risse, H.-J. Freund, G. Pacchioni, and A. Scagnelli, *Phys. Rev. Lett.* **96**, 146804 (2006).
- ¹⁴M. Sterrer, M. Yulikov, T. Risse, H.-J. Freund, J. Carrasco, F. Illas, C. di Valentin, L. Giordano, and G. Pacchioni, *Angew. Chem., Int. Ed.* **45**, 2633 (2006).
- ¹⁵G. Barcaro and A. Fortunelli, *Phys. Rev. B* **76**, 165412 (2007).
- ¹⁶G. Barcaro, M. Causa, and A. Fortunelli, *Theor. Chem. Acc.* **118**, 807 (2007).
- ¹⁷G. Barcaro and A. Fortunelli, *J. Phys. Chem. C* **111**, 11384 (2007).
- ¹⁸G. Barcaro, E. Apra, and A. Fortunelli, *Chem.-Eur. J.* **13**, 6408 (2007).
- ¹⁹G. Barcaro, A. Fortunelli, G. Rossi, F. Nita, and R. Ferrando, *Phys. Rev. Lett.* **98**, 156101 (2007).
- ²⁰G. Barcaro and A. Fortunelli, *New J. Phys.* **9**, 22 (2007).
- ²¹J. Oviedo, J. Fernandez-Sanz, N. López, and F. Illas, *J. Phys. Chem. B* **104**, 4342 (2000).
- ²²A. V. Matveev, K. M. Neyman, I. V. Yudanov, and N. Rösch, *Surf. Sci.* **426**, 123 (1999).
- ²³A. V. Matveev, K. M. Neyman, G. Pacchioni, and N. Rösch, *Chem. Phys. Lett.* **299**, 603 (1999).
- ²⁴A. Bogicevic and D. R. Jennison, *Surf. Sci.* **437**, L741 (1999).
- ²⁵H. Gronbeck and P. Broqvist, *J. Chem. Phys.* **119**, 3896 (2003).
- ²⁶K. M. Neyman, S. Vent, G. Pacchioni, and N. Rösch, *Nuovo Cimento Soc. Ital. Fis., D* **19**, 1743 (1997).
- ²⁷I. Yudanov, G. Pacchioni, K. Neyman, and N. Rösch, *J. Phys. Chem. B* **101**, 2786 (1997).
- ²⁸N. López, F. Illas, N. Rösch, and G. Pacchioni, *J. Chem. Phys.* **110**, 4873 (1999).
- ²⁹N. Lopez and F. Illas, *J. Phys. Chem. B* **102**, 1430 (1998).
- ³⁰D. Matsunaka and Y. Shibutani, *Phys. Rev. B* **77**, 165435 (2008).
- ³¹F. Cinquini, C. di Valentin, E. Finazzi, L. Giordano, and G. Pacchioni, *Theor. Chem. Acc.* **117**, 827 (2007).
- ³²L. Giordano, G. Pacchioni, A. M. Ferrari, F. Illas, and N. Rösch, *Surf. Sci.* **473**, 213 (2001).
- ³³A. del Vitto, C. Sousa, F. Illas, and G. Pacchioni, *J. Chem. Phys.* **121**, 7457 (2004).
- ³⁴A. Markovits, J. C. Paniagua, N. López, C. Minot, and F. Illas, *Phys. Rev. B* **67**, 115417 (2003).
- ³⁵L. Xu, G. Henkelman, C. T. Campbell, and H. Jónsson, *Phys. Rev. Lett.* **95**, 146103 (2005).
- ³⁶G. Pacchioni, *ChemPhysChem* **4**, 1041 (2003).
- ³⁷N. López, J. C. Paniagua, and F. Illas, *J. Chem. Phys.* **117**, 9445 (2002).
- ³⁸G. Pacchioni, A. M. Ferrari, A. M. Marquez, and F. Illas, *J. Comput. Chem.* **18**, 617 (1997).
- ³⁹O. Robach, G. Renaud, and A. Barbier, *Phys. Rev. B* **60**, 5858 (1999).
- ⁴⁰A. D. Becke, *J. Chem. Phys.* **98**, 5648 (1993); C. Lee, W. Yang, and R. G. Parr, *Phys. Rev. B* **37**, 785 (1988).
- ⁴¹M. J. Frisch *et al.*, GAUSSIAN 03, Revision C.02, Gaussian, Inc.,

- Wallingford CT, 2004.
- ⁴²F. Illas, I. de P. R. Moreira, C. de Graaf, and V. Barone, *Theor. Chem. Acc.* **104**, 265 (2000).
- ⁴³F. Illas, I. de P. R. Moreira, J. M. Bofill, and M. Filatov, *Theor. Chem. Acc.* **116**, 587 (2006).
- ⁴⁴I. de P. R. Moreira, R. Costa, M. Filatov, and F. Illas, *J. Chem. Theory Comput.* **3**, 764 (2007).
- ⁴⁵P. S. Bagus and B. I. Bennet, *Int. J. Quantum Chem.* **9**, 143 (1975).
- ⁴⁶T. Ziegler, A. Rauk, and E. J. Baerends, *Theor. Chim. Acta* **43**, 261 (1977).
- ⁴⁷C. Sousa, G. Pacchioni, and F. Illas, *Surf. Sci.* **429**, 217 (1999).
- ⁴⁸M. Chiesa, M. C. Paganini, E. Giamello, C. Di Valentin, and G. Pacchioni, *Acc. Chem. Res.* **39**, 861 (2006).
- ⁴⁹D. Ricci, C. Di Valentin, G. Pacchioni, P. V. Sushko, A. L. Shluger, and E. Giamello, *J. Am. Chem. Soc.* **125**, 738 (2003).
- ⁵⁰A. Reed, R. B. Weinstock, and F. Weindhold, *J. Chem. Phys.* **83**, 735 (1985).
- ⁵¹A. M. Ferrari and G. Pacchioni, *J. Phys. Chem.* **100**, 9032 (1996).
- ⁵²C. DiValentin, L. Giordano, G. Pacchioni, and N. Rosch, *Surf. Sci.* **522**, 175 (2003).
- ⁵³E. Florez, F. Mondragon, T. N. Truong, and P. Fuentealba, *Phys. Rev. B* **73**, 115423 (2006).
- ⁵⁴Y. Wang, E. Florez, F. Mondragon, and T. N. Truong, *Surf. Sci.* **600**, 1703 (2006).
- ⁵⁵K. M. Neyman, C. Inntam, A. V. Matveev, V. A. Nasluzov, and N. Rösch, *J. Am. Chem. Soc.* **127**, 11652 (2005).
- ⁵⁶K. H. Hansen, T. Worren, S. Stempel, E. Laegsgaard, M. Bäumer, H.-J. Freund, F. Besenbacher, and I. Stensgaard, *Phys. Rev. Lett.* **83**, 4120 (1999).
- ⁵⁷M. Bäümer and H.-J. Freund, *Prog. Surf. Sci.* **61**, 127 (1999).
- ⁵⁸S. Stempel, M. Bäümer, and H.-J. Freund, *Surf. Sci.* **402-404**, 424 (1998).
- ⁵⁹G. Pacchioni, in *Theory of Metal Clusters on the MgO Surface: The Role of Point Defects in Nanocatalysis*, edited by U. Heiz and U. Landmand (Springer, Berlin, 2007).